Scientia Iranica A (2016) 23(1), 21–35

Sharif University of Technology
Scientia Iranica
Transactions A: Civil Engineering
www.scientiairanica.com

Shape optimization of concrete arch dams considering stage construction

S. Pourbakhshian[a], M. Ghaemian[b,*] and A. Joghataie[b]

a. *Department of Civil Engineering, Science and Research Branch, Islamic Azad University, Tehran, Iran.*
b. *Department of Civil Engineering, Sharif University of Technology, Tehran, Iran.*

Received 30 October 2013; received in revised form 14 June 2014; accepted 20 October 2014

KEYWORDS
Arch dam;
Shape optimization;
Stage construction;
Simultaneous perturbation stochastic approximation;
Cubic spline.

Abstract. This paper describes a methodology to develop the interface between a finite element software and optimization algorithm for optimization of concrete high arch dams. The objective function is the volume of the dam. The numbers of design variables are 31 including the thickness and upstream profile of crown cantilever, thickness of the left and right abutments, radius of curvature of water and air faces left and right by use of polynomial curve fitting and cubic spline function. The constraint conditions are the geometric shape, stress, and the stability against sliding. Initially, a program is developed in MATLAB in order to generate the coordinates of nodes; then, finite element software ANSYS is taken for modeling the geometry of dam. Finally, the optimization technique is performed by Simultaneous Perturbation Stochastic Approximation algorithm. To include dead weight of dam body, stage construction is considered. The proposed method is applied successfully to an arch dam and good results are achieved. The results indicate that the concrete volume of the optimized dam is reduced by an average of 21%. Compared with the initial shape, the time of convergence in this method is very short and the method is fairly effective. It can be applied to practical engineering design.

1. Introduction

The optimal shape is the best design for a structure subject to various constraints imposed by the restrictions placed on the design. Shape optimization is the key step in the design of an arch dam.

The geometrical shape defined during the initial design phase is not always the best one from technical and economical points of view. The best shape should be defined by means of optimization studies, which employ a set of structural safety and minimal cost criteria [1]. Introduction to Optimum Design started from the late 1960's and several different researchers continued it [2-22]. In recent years, many methods of optimization are being developed rapidly and much attention has been paid by several authors to the fields of concrete arch dam.

Sun et al. [23] established an optimization model for the shape design of arch dam by the use of cubic spline arch for the shape parameters, such as the coordinates of nodes, semi-center angle, and the thickness of arch abutment. The results indicated that the concrete volume of the arch dam optimized by the proposed cubic spline was less than the original design scheme optimized using parabolic shape. Li et al. [24] used the modified complex method which can search for the optimal solution directly, has no special request on the condition of the objective function and constraint function, and does not need to derivate during iteration pilot calculation. Fanelli [25] showed that the degrees of

*. *Corresponding author. Tel.: +98 21 66164242*
E-mail addresses: spourbakhshiyan@iauramsar.ac.ir (S. Pourbakhshian); ghaemian@sharif.edu (M. Ghaemian)

freedom, which are strictly necessary to be considered in the shape optimization procedure of an arch dam, can be reduced by a judicious choice of basic model and design variables. Peng et al. [26] expressed that the optimization of arch dams is complex, because its objective function and constraint conditions appear non-linear and it applies a genetic algorithm with closure temperature field for shape optimization of arch dams.

Tajalli et al. [27] used Bofang formulation for parabolic arch dam. The finite element analysis and optimization procedure are implemented by commercial programs. The combination of Simultaneous Perturbation Stochastic Approximation (SPSA) and Particle Swarm Optimization (PSO) algorithm is introduced by Hamidian et al. [28] to find the optimal shapes of arch dams. Akbari et al. [29] employed a new algorithm for geometry modeling of arch dams using Hermit cubic splines and the optimization problem solved via the Sequential Quadratic Programming (SQP) method. Takalloozadeh and Ghaemian [30] did the shape optimization of arch dams considering abutment stability with Particle Swarm Optimization (PSO) method.

The present study describes a method for shape optimization of double curvature concrete arch dam. In the optimization process, the objective function is volume of the concrete arch dam. Design variables of processing are the geometric shape parameters of the double curvature of arch dam and the constraint conditions are geometric shape, stress, and stability against sliding. The program basically consists of three parts that are described in the paper:

1. Generation of the coordinate of nodes by MATLAB code;
2. Call ANSYS batch file for analysis;
3. Optimization of the arch dams by SPSA algorithm according to the established load combination.

For optimization purposes, it is convenient to consider the effects of dam body dead weight and upstream hydrostatic pressures. To include dead weight of dam body, stage construction is considered. The proposed method is successfully applied to an arch dam, where good results are achieved. The results indicate that the concrete volume of the optimized arch dam is reduced by an average of 21%. Compared with the initial shape, the time of convergence in this method is very short and the method is fairly effective. It can be applied to practical engineering design.

2. Mathematical equation of arch dam design

2.1. Preliminary design

The main geometric parameters of the arch dam are shown in Table 1.

Table 1. The main geometric parameters.

K	Arch number
EL	Elevation
T_C	Thickness of the crown cantilever
T_{AL}	Left abutment thickness
T_{AR}	Right abutment thickness
USP	Crown cantilever upstream profile
DSP	Crown cantilever downstream profile
R_{LUS}	Radius of curvature of left water face
R_{RUS}	Radius of curvature of right water face
R_{LDS}	Radius of curvature of left air face
R_{RDS}	Radius of curvature of right air face
x_{eL}	Left abetment curve
x_{eR}	Right abetment curve

2.2. The geometric model of an arch dam

The shape of an arch dam is of paramount importance in its ultimate behavior and eventually settles all design criteria. Variable curvature arch dams evolved to be economical in shape optimization studies [31].

These geometrical parameters can be defined as follows.

2.2.1. Crown cantilever shape

For definition of crown cantilever, two quadratic functions of vertical coordinates for water and air face are employed.

$$\mathrm{USP}(Z) = a_0 + a_1 Z + a_2 Z^2, \tag{1}$$

$$\mathrm{DSP}(Z) = b_0 + b_1 Z + b_2 Z^2, \tag{2}$$

in which Z is vertical coordinate; a_0, a_1, a_2, and b_0, b_1, b_2 are the coefficients, and extrude is the curved upstream surface of the horizontal arch elements. The intrados is the curved downstream surface of horizontal arch elements; USP and DSP are the crown cantilever U/S (upstream) and D/S (downstream) profile, respectively. In other words, USP is the horizontal distance between the extrados and the axis on a line normal to the extrados and the DSP is the horizontal distance between the intrados and the axis on a line normal to the intrados. In Figure 1, the shape of crown cantilever and layers at control elevations are shown.

2.2.2. Thickness of arch dam

In this paper, the variations of thicknesses of the vertical crown cantilever and the horizontal arch sections are taken to be the third-degree polynomials of the vertical coordinate. The thicknesses of the arch horizontal sections are calculated using the following equations:

$$t_c(Z) = c_0 + c_1 Z + c_2 Z^2 + c_3 Z^3, \tag{3}$$

$$t_{AL}(Z) = d_0 + d_1 Z + d_2 Z^2 + d_3 Z^3, \tag{4}$$

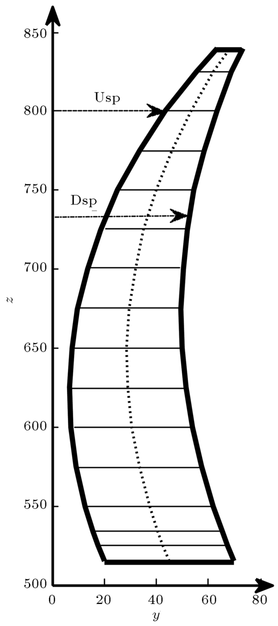

Figure 1. Cross section of crown cantilever.

$$t_{AR}(Z) = e_0 + e_1 Z + e_2 Z^2 + e_3 Z^3, \tag{5}$$

in which $t_c(Z)$, $t_{AL}(Z)$, and $t_{AR}(Z)$ are the crown, left, and right abutment thicknesses, respectively. Z is vertical coordinate and $c_0, ..., c_3$, $d_0, ..., d_3$, and $e_0, ..., e_3$ are the coefficients. In this way, the downstream profile can be written in the following form:

$$\mathrm{DSP} = \mathrm{USP} \ + t_c. \tag{6}$$

2.2.3. Radius of curvature

The cubic spline is used to define the radii of curvature of water and air faces. The number of horizontal arch layers is selected as 16 from the base to the crest elevation (Figure 1).

The radius of curvature R is specified at interpolation points by R_1, R_7, R_{11}, R_{16} (R_{LUS1}, R_{LUS7}, R_{LUS11}, R_{LUS16}, R_{RUS1}, R_{RUS7}, R_{RUS11}, R_{RUS16}, R_{LDS1}, R_{LDS7}, R_{LDS11}, R_{LDS16}, R_{RDS1}, R_{RDS7}, R_{RDS11}, R_{RDS16}) as design variables. R is interpolated at each level with the following cubic spline (Figure 2).

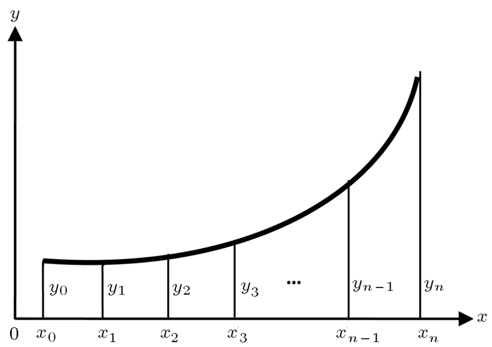

Figure 2. Cubic spline.

Given the following list of points:

$$a = x_0 < x_1 <, ..., < x_n = b \rightarrow \quad x \in |x_i, x_{i+1}| \rightarrow$$

$$(i = 0, 1, ..., n-1)$$

$$y_0 \ y_1 \ , ..., y_n. \tag{7}$$

A cubic spline $S(x)$ is a piecewise-defined function that satisfies the following conditions:

1. $S(x) = S_i(x)$ is a cubic polynomial on each subinterval:
$$[x_i, x_{i+1}] \qquad (i = 0, 1, ..., n-1), \tag{8}$$
2. $S(x_i) = y_i \ \ i = 0, 1, ..., n,$ (9)
S interpolates all the points.
3. $S(x)$, $S'(x)$, and $S''(x)$ are continuous on $[a, b]$ (S is smooth).

So, the n cubic polynomial pieces can be written as:

$$S_i(x) = a_i + b_i(x - x_i) + c_i(x - x_i)^2 + d_i(x - x_i)^3,$$

$$i = 0, 1, ..., n-1, \tag{10}$$

in which a_i, b_i, c_i, and d_i represent $4n$ unknown coefficients. The following conditions are held for interpolation and continuity:

a) $S(x)$ is continuous at discrete points:
$$S_i(x_i) = y_i, \qquad i = 0, 1, ..., n-1, \tag{11}$$
$$S_i(x_{i+1}) = y_{i+1}, \qquad i = 0, 1, ..., n-1. \tag{12}$$

b) Derivatives of $S(x)$ at discrete points are:
$$S_i'(x_{i+1}) = S_{i+1}'(x_{i+1}) \quad i = 0, 1, ..., n-2, \tag{13}$$
$$S_i''(x_{i+1}) = S_{i+1}''(x_{i+1}), \quad i = 0, 1, ..., n-2. \tag{14}$$

Based on conditions (a) and (b), the total number of equations is $4n - 2$. The expressions for the derivatives of S_i can be written as:

$$S_i(x) = a_i + b_i(x - x_i) + c_i(x - x_i)^2 + d_i(x - x_i)^3, \tag{15}$$

$$S_i'(x) = b_i + 2c_i(x - x_i) + 3d_i(x - x_i)^2, \tag{16}$$

$$S_i''(x) = 2c_i + 6d_i(x - x_i). \tag{17}$$

If $h_i = x_{i+1} - x_i$, then the spline conditions can be written as follow (substitute Eqs. (11) to (14) into Eqs. (15) to (17)):

$$a_i = y_i, \tag{18}$$

$$a_i + h_i b_i + h_i^2 c_i + h_i^3 d_i = y_{i+1}, \tag{19}$$

$$b_i + 2h_ic_i + 3h_i^2d_i - b_{i+1} = 0, \tag{20}$$

$$2c_i + 6h_id_i - 2c_{i+1} = 0. \tag{21}$$

The above equations can be written as a linear system for the $4n$ unknowns, i.e. a_0, b_0, c_0, d_0, a_1, b_1, c_1, d_1,..., a_{n-1}, b_{n-1}, c_{n-1}, d_{n-1}.

The definition of term m_i is given in Eq. (22):

$$S_i''(x_i), ..., S_i''(x_i) = 2c_i \quad \text{or} \quad c_i = m_i/2. \tag{22}$$

Considering m_i as unknowns instead, we have (substitute Eqs. (22) and (14) into Eq. (21)):

$$d_i = (m_{i+1} - m_i)/(6h_i). \tag{23}$$

Substitute Eqs. (11) and (12) into Eq. (19) in the following:

$$y_i + h_ib_i + h_i^2c_i + h_i^3d_i = y_{i+1}. \tag{24}$$

Substituting c_i and d_i from Eqs. (22) and (23) into Eq. (21), the following is obtained:

$$b_i = \frac{y_{i+1} - y_i}{h_i} - \frac{h_i}{2}m_i - \frac{h_i}{6}(m_{i+1} - m_i).$$

From Eq. (13) we have:

$$b_i + 2h_ic_i + 3h_i^2d_i = b_{i+1}. \tag{25}$$

Substitute Eqs. (22), (23) and (25) into Eq. (21):

$$h_im_i + 2(h_i + h_{i+1})m_{i+1} + h_{i+1}m_{i+2}$$
$$= 6\left[\frac{y_{i+2} - y_{i+1}}{h_{i+1}} - \frac{y_{i+1} - y_i}{h_i}\right]. \tag{26}$$

These are $(n-1)$ linear equations for $(n+1)$ unknowns, i.e. $m_0, m_1, m_2, \ldots, m_n$, where $m_i = g_i''(x_i)$.

For taken together gives an $(n+1)\times(n+1)$ system of equation as shown in Box I.

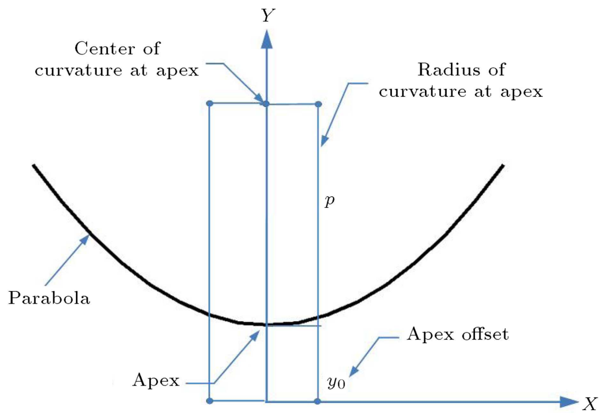

Figure 3. Parabola definition.

2.2.4. Horizontal arches

For definition of dam geometry in horizontal sections, parabolic conic functions are employed (Figure 3). The general equation of water and air face parabolas is:

$$\begin{cases} ax^2 + bxy + cx^2 + dx + ey + f = 0 \\ \Delta = 4ac - b^2 \\ \Delta < 0 \quad \text{hyperbola} \\ \Delta > 0 \quad \text{ellipse} \\ \Delta = 0 \quad \text{parabola} \end{cases} \tag{28a}$$

Corresponding coefficients of general conic function shall be as follows:

$$\begin{cases} a = 1 \\ b = 0 \\ c = 0 \qquad\qquad \Rightarrow y = y_0 + \frac{(x-x_0)^2}{2p} \\ d = -2x_0 \\ e = -2p \\ f = x_0^2 + 2py_0 \end{cases} \tag{28b}$$

In Figure 3, some related details and geometric parameters, used to define a general horizontal parabolic arch, are shown. Each parabola is defined by the position of its apex (y_0) and its radius of curvature at the apex. In water face, y_0=USP, and the radius of curvature are

$$\begin{bmatrix} 1 & 0 & 0 & \cdots & 0 \\ h_0 & 2(h_0+h_1) & h_1 0 & \cdots & 0 \\ 0 & h_1 & 2(h_1+h_2)h_2 & \cdots & 0 \\ 0 & 0 & h_2 2(h_2+h_3) & h_3 & 0 \\ \vdots & & \ddots\ddots & \ddots & \vdots \\ 0 & & h_{n-2} & 2(h_{n-2}+h_{n-1}) & h_{n-1} \\ 0 & \cdots & 0 & 0 & 1 \end{bmatrix} \begin{bmatrix} m_0 \\ m_1 \\ m_2 \\ m_3 \\ \vdots \\ m_n \end{bmatrix} = 6 \begin{bmatrix} 0 \\ \frac{y_2-y_1}{h_1} - \frac{y_1-y_0}{h_0} \\ \frac{y_3-y_2}{h_1} - \frac{y_2-y_1}{h_1} \\ \frac{y_4-y_3}{h_1} - \frac{y_3-y_2}{h_2} \\ . \\ . \\ \frac{y_n-y_{n-1}}{h_{n-1}} - \frac{y_{n-1}-y_{n-2}}{h_{n-1}} \end{bmatrix} \tag{27}$$

If $m_0 = 0$, $m_n = 0$, the above equation system will be reduced to $(n+1)\times(n+1)$ system.

Box I

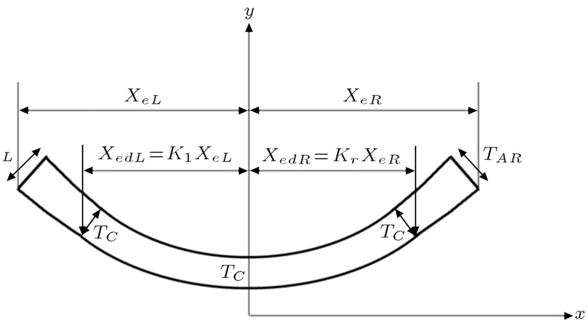

Figure 4. A horizontal arch of the dam body.

RLUS and RRUS. In air face, $y_0 =$ DSP, and the radius of curvature are RLDS and RRDS. Again, the radii of curvature at apex point are defined by spline. The axes of three parabolas are coincident and are positioned on dam reference plane.

To define the horizontal section, two parabolic curves are defined in the left and right sides of Figure 4. This is done in order to model an unsymmetrical arch dam. Each side is divided into two segments: constant thickness and variable thickness. The thickness of the dam in horizontal section is constant in the first segment and increases by parabolic function in the second one [32]. Coefficients k_r and k_l determine portion of the length of arch with constant thickness in the right and left banks. In this paper, k_r and k_l are equal to 2/3.

$$\begin{cases} \text{For the right half} \\ T_{aR}(x) = T_C + \frac{(x-x_{edR})^2(T_{AR}-T_C)^2}{(x_{eR}-x_{edR})^2} \\ \qquad x_{edR} < x < x_{eR} \\ T_{aR} = T_C \qquad x < x_{edR} \\ \text{For the left half} \\ T_{aL}(x) = T_C + \frac{(x-x_{edL})^2(T_{AL}-T_C)^2}{(x_{eL}-x_{edL})^2} \\ \qquad x_{edL} < x < x_{eL} \\ T_{aL} = T_C \qquad x < x_{edL} \end{cases} \tag{29}$$

x_{edL} and x_{edR} are lengths of segments with constant thicknesses in the left and right banks, respectively (Figure 4).

Difference in the x coordinates of the upstream surface corresponds to 25 meters (Δx).

The number of horizontal arch layers is selected as 16 from the base to the crest elevation. This can be selected based on dam elevation for each layer. In Table 1, the basic input parameters for definition of crown cantilever and horizontal arches are included. The x coordinate of the vertical middle line can be calculated from the x coordinate of the upstream (x_{eu}) and downstream surface (x_{id}), which can be written as:

$$\frac{x_{eu} + x_{id}}{2}. \tag{30}$$

2.2.5. Programming and implementation of 3D model and loadings

According to the above formula, a MATLAB program for geometrical design of arch dams was written so that Finite element model was developed in the APDL programming language of the ANSYS code. In finite element modeling of the arch dam, geometry is considered as doubled curvature arch dam. In the finite element model of an arch dam, 1580 eight-node elements in the foundation and 180 twenty-node elements in the dam body are used. Each node has three degrees of freedom: translations in the nodal X, Y and Z directions. Two layers of elements were set along thickness of the dam. The finite element model of the dam is developed so that it includes the foundation. As it is shown in Figure 4, the length and width of the foundation along the global X and Y axes are taken to be 1650 m. For the 3D arch dam analysis, mass concrete and rock were assumed to be homogeneous with linear elastic materials. The modulus of elasticity of mass concrete was taken as 28 GPa and that of the foundation rock as 9 GPa. The Poisson's ratios of mass concrete and rock were taken as 0.18 and 0.25, respectively. Mass density of the concrete was chosen as 2400 kg/m^3 and no gravity load was applied on the foundation rock. Concrete and rock were assumed to be homogeneous and isotropic materials. As the foundation is assumed as massless, only the effects of foundation flexibility are considered in the analysis. For the boundary conditions in the finite element model of the dam, all degrees of freedom are fixed at the outside surfaces of the foundation.

Figure 5 illustrates the dam, foundation, and reservoir finite element model. The usual static cases include the effects of silt and tail water pressures and temperature (either summer or winter), while for optimization purposes, it is convenient to exclude all these effects and merely consider the effects of dam body dead weight and upstream hydrostatic pressures. In this research, two basic loading cases, as follows, have been considered for the optimization procedure:

1. SU1 (the first usual static load combination) or self-weight;
2. SUN1 (the first unusual static unusual load com-

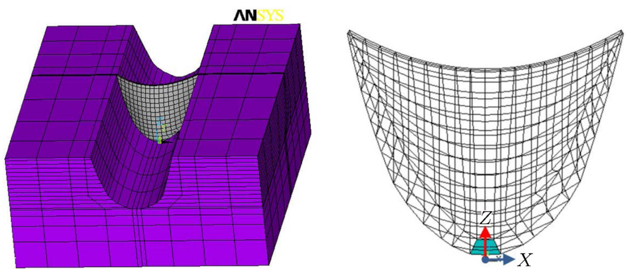

Figure 5. Three-dimensional shape of an arch dam with foundation.

Table 2. Load combinations used for presenting the analyses results.

Load combination number	Single load parts		Factor of safety		Load combination
	Dead weight	Normal water pressure	Tension	Compression	
SU1	√	√	2	3	Static usual
SUN1	√	-	1.5	2	Static unusual

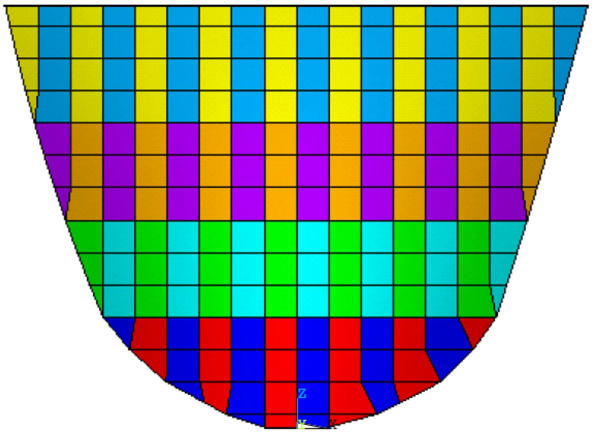

Figure 6. Construction stages.

bination) or self-weight and upstream hydrostatic pressures.

Two different load combinations are listed in Table 2.

As the self-weight considered by staged construction method in which dead load is applied in several stages.

As shown in Figure 6, self-weight simulation is carried out in 8 stages. Indeed, it is assumed that each stage corresponds to a lift of concrete. The lift height is taken equal to the vertical distance between two consecutive horizontal arches enclosing one row of finite elements in the model. The element birth option of the ANSYS program is adequately utilized to resemble addition of finite elements i.e. concrete lifts to the whole model. The birth time of the elements of any specific lift corresponds to the placement time of that lift. The placement time is just a fictitious number and does not intend to resemble the real practical situation. It is worth to mention that the whole concrete of each lift (one stage) is assumed to be placed simultaneously.

3. The optimization method of arch dam shape

Shape optimization aims to minimize consumed concrete volume while enhancing safety criteria. The shape optimization problem is to find the design variable X while minimizing the objective function $F(x)$ under the constraint functions $h_j(X)$ and $g_j(X)$ that can be stated mathematically as:

$$\text{Find} \quad X = [X_1, X_2, ..., X_n]^T,$$

$$a_i \leq X \leq b_i \quad (i = 1, 2, ..., n).$$

$$\text{To minimize} \quad F(x)$$

$$h_j(X) = 0 \quad (j = 1, 2, ..., p),$$

$$g_k(X) \leq 0 \quad (k = 1, 2, ..., m). \tag{31}$$

The subscripts p, m, and n denote the number of equality constraints, behavioral constraints, and design variables, respectively, where a_i and b_i are allowable lower and upper limits of the design variables, which are introduced to deal with various requirements.

3.1. Design variables

Shape optimization can be improved by increasing the number of design variables, but it raises the cost of calculations. According to the geometrical model of arch dams described before in the paper, the design variables can be selected as: 31 design variables, which will be used in the process of optimization, as shown in Table 3.

Crown cantilever design variables are shown in Figure 7.

3.2. Objective function

The purpose of optimization is to choose proper geometric shape of arch dam to make the project cost minimal on the premise of meeting the needs of

Table 3. Design variables.

Thickness			Radius				USP
t_{C1}	t_{AL1}	t_{AR1}	R_{LUS1}	R_{RUS1}	R_{LDS1}	R_{RDS1}	USP_1
t_{C7}	t_{AL7}	t_{AR7}	R_{LUS7}	R_{RUS7}	R_{LDS7}	R_{RDS7}	USP_7
t_{C11}	t_{AL11}	t_{AR11}	R_{LUS11}	R_{RUS11}	R_{LDS11}	R_{RDS11}	USP_{16}
t_{C16}	t_{AL16}	t_{AR16}	R_{LUS16}	R_{RUS16}	R_{LDS16}	R_{RDS16}	

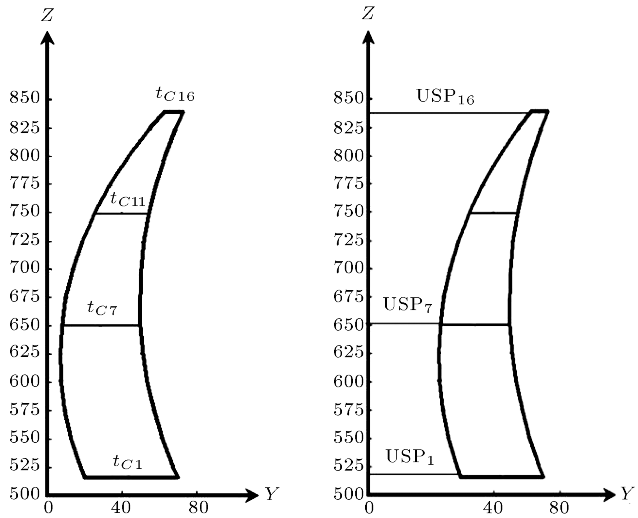

Figure 7. Crown cantilever design variables.

strength and stability. Generally, the cost of arch dam is mainly dependent upon the volume of dam body concrete. So, the objective function is the dam body volume.

3.3. Constraint functions

In shape optimization of concrete arch dams, the following three types of constraint sets should be satisfied, as required by the demands of design and construction:

1. Geometrical constraints;
2. Stress constraints;
3. Stability constraints.

3.3.1. Geometrical constraints set

Thickness of horizontal arch: The thickness of crown cantilever decreases from base to the dam crest.

$$T_{C_{i+1}} < T_{C_i} \rightarrow \frac{T_{C_{i+1}}}{T_{C_i}} - 1 \leq 0 \quad (i = 0, 1, ..., n). \quad (32)$$

For different elevations, the crown cantilever thickness is lower than abutment thickness.

$$T_{C_i} < T_{AR_i} \rightarrow \frac{T_{C_i}}{T_{AR_i}} - 1 \leq 0 \quad (i = 0, 1, ..., n), \quad (33)$$

$$T_{C_i} < T_{AL_i} \rightarrow \frac{T_{C_i}}{T_{AL_i}} - 1 \leq 0 \quad (i = 0, 1, ..., n). \quad (34)$$

Slope of overhang in upstream and downstream of arch dam: To facilitate construction, the maximum slope of overhang at the upstream and downstream faces should be controlled as follows (Figure 8).

Below tangent points, the angles of tangents are negative and above it, they are positive. The plotting steps should be increased to avoid gap in curves of the upper and lower parts.

$$\theta^U_{\max} \leq \theta^U_{alw}, \quad (35)$$

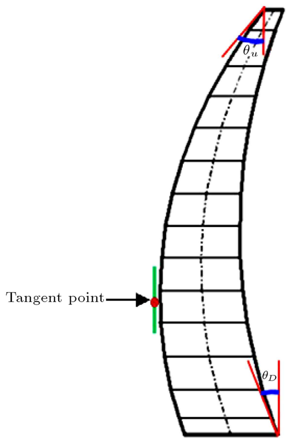

Figure 8. The slope of overhang in upstream and downstream of arch dam.

$$\theta^D_{\max} \leq \theta^D_{alw}, \quad (36)$$

where $\theta^U_{\max}$ and $\theta^D_{\max}$ are the allowable maximal overhang slopes of the upstream and downstream surfaces, and θ^U_{alw} and θ^D_{alw} are the allowable maximal overhang slopes, respectively.

Crown cantilever profile: Below tangent points, the angles of tangents are negative and above it, they are positive. The plotting steps should be increased to avoid gap in curves of the upper and lower parts.

Crown cantilever upstream profile:

$$\mathrm{USP}_{i+1} < \mathrm{USP}_i \rightarrow \frac{\mathrm{USP}_{i+1}}{\mathrm{USP}_i} - 1 \leq 0$$

$$(i = 0, 1, ..., n_{\text{tangent point}}, ..., n), \quad (37)$$

$$\mathrm{USP}_i < \mathrm{USP}_{i+1} \rightarrow \frac{\mathrm{USP}_i}{\mathrm{USP}_{i+1}} - 1 \leq 0$$

$$(i = n_{\text{tangent point}}, ..., n). \quad (38)$$

Crown cantilever downstream profile:

$$\mathrm{DSP}_{i+1} < \mathrm{DSP}_i \rightarrow \frac{\mathrm{DSP}_{i+1}}{\mathrm{DSP}_i} - 1 \leq 0$$

$$(i = 0, 1, ..., n_{\text{tangent point}}, ..., n), \quad (39)$$

$$\mathrm{DSP}_i < \mathrm{DSP}_{i+1} \rightarrow \frac{\mathrm{DSP}_i}{\mathrm{DSP}_{i+1}} - 1 \leq 0$$

$$(i = n_{\text{tangent point}}, ..., n). \quad (40)$$

Location of the tangent point: As shown in Figure 9, the maximum distance between crest and tangent point is 0.6 H [33].

$$H_{\text{Tangant point}_{\max}} = 0.6H, \quad (41)$$

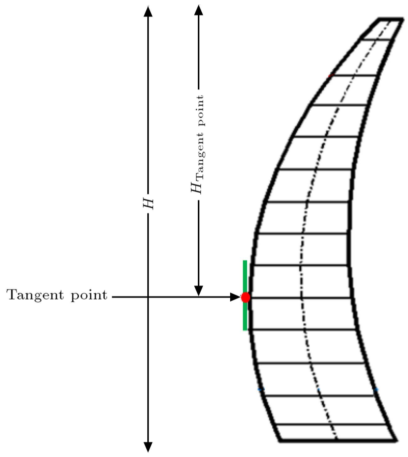

Figure 9. Location of the tangent point.

$$H_{\text{Tangent point}} < H_{\text{Tangent point}_{\max}} \rightarrow \frac{H_{\text{Tangent point}}}{H_{\text{Tangent point}_{\max}}} - 1 \leq 0. \quad (42)$$

Radius of curvature. The most important geometric constraints are those that prevent intersection of upstream and downstream faces as:

$$R_{\text{LDS}_i} < R_{\text{LUS}_i} \rightarrow \frac{R_{\text{LDS}_i}}{R_{\text{LUS}_i}} - 1 \leq 0 \quad (i = 0, 1, ..., n), \quad (43)$$

$$R_{\text{RDS}_i} < R_{\text{RUS}_i} \rightarrow \frac{R_{\text{RDS}_i}}{R_{\text{RUS}_i}} - 1 \leq 0 \quad (i = 0, 1, ..., n). \quad (44)$$

The variation of radius at crown cantilever along with height of dam should be satisfactory to some kind of nonlinear variation rule.

$$R_{\text{LUS}_i} < R_{\text{LUS}_{i+1}} \rightarrow \frac{R_{\text{LUS}_i}}{R_{\text{LUS}_{i+1}}} - 1 \leq 0 \quad (i = 0, 1, ..., n), \quad (45)$$

$$R_{\text{RUS}_i} < R_{\text{RUS}_{i+1}} \rightarrow \frac{R_{\text{RUS}_i}}{R_{\text{RUS}_{i+1}}} - 1 \leq 0 \quad (i = 0, 1, ..., n), \quad (46)$$

$$R_{\text{RDS}_i} < R_{\text{RDS}_{i+1}} \rightarrow \frac{R_{\text{RDS}_i}}{R_{\text{RDS}_{i+1}}} - 1 \leq 0 \quad (i = 0, 1, ..., n), \quad (47)$$

where R_{RUS_i} and R_{RDS_i} are radius of curvatures at the upstream and downstream faces of the dam in the ith layer in z direction.

3.3.2. Stress constraints

Stress constraints are used to control stress distribution in the structure. Under different loads imposed on arch dam, the maximum stress is less than the allowable stress. In this study, the behavior constraints are defined to prevent failure of each element (i) of arch dam under specified safety factor (sf). For this purpose, the failure criterion of concrete of Willam and Warnke [32] due to multiaxial stress state is employed as follows:

$$\frac{f}{f_c} \leq \frac{s}{sf} \rightarrow \frac{f}{f_c} - \frac{s}{sf} \leq 0 \quad (i = 0, 1, ..., n_e), \quad (48)$$

where (f) is a function of the principal stress state ($\sigma_1 \geq \sigma_2 \geq \sigma_3$) and ($s$) is failure surface expressed in terms of principal stresses, uniaxial compressive strength of concrete (f_c), uniaxial tensile strength of concrete (f_t), and biaxial compressive strength of concrete (f_{cb}). Table 4 shows the four principal stress states by which the failure of concrete is categorized into four domains. In each domain, independent functions describe (f) and the failure surface (s). The details of failure criterion can be found in Willam and Warnke and the theory reference of ANSYS.

The angle of similarity (η) describes the relative magnitudes of the principal stresses as:

$$\cos\eta = \frac{2\sigma_1 - \sigma_2 - \sigma_3}{\sqrt{2}\left[(\sigma_1 - \sigma_2)^2 + (\sigma_2 + \sigma_3)^2 + (\sigma_3 - \sigma_1)^2\right]^{1/2}}. \quad (49)$$

The parameters (r_1) and (r_2) represent the failure surface of all stress states with ($\eta = 0°$) and ($\eta = 60°$), respectively, and they are functions of principal stresses and concrete strengths. The parameters (r_1) and (r_2) and the angle (η) are shown in Figure 10.

Therefore, Eq. (40) must be checked for the center of all dam elements (n_e) with safety factor that is chosen as $sf = 1$. If it is satisfied, there is no crack or crush. Otherwise, the material will crack if any principal stress is tensile, while crushing will occur if all principal stresses are compressive.

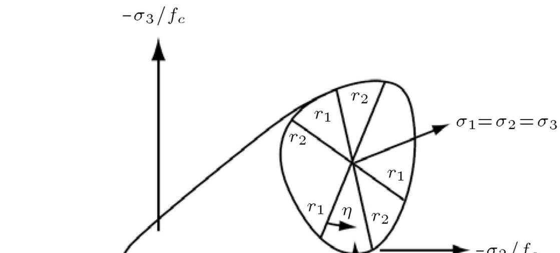

Figure 10. Failure surface in the compression-compression-compression Regime.

Table 4. The equation of Willam and Warnke.

Domain	(f, s)
Compression Compression Compression	$f = \frac{1}{\sqrt{15}}\left[(\sigma_1-\sigma_2)^2+(\sigma_2-\sigma_3)^2+(\sigma_3-\sigma_1)^2\right]^{1/2}$ $s = \frac{2r_2(r_2^2-r_1^2)\cos\eta+r_2(2r_1-r_2)\left[4(r_2^2-r_1^2)\cos^2\eta+5r_1^2-4r_1r_2\right]^{1/2}}{4(r_2^2-r_1^2)\cos^2\eta+(r_2-2r_1)^2}$
Tension Compression Compression	$f = \frac{1}{\sqrt{15}}\left[(\sigma_2)^2+(\sigma_2-\sigma_3)^2+\sigma_3^2\right]^{1/2}$ $s = \left(1-\frac{\sigma_1}{f_t}\right)\frac{2p_2(p_2^2-p_1^2)\cos\eta+p_2(2p_1-p_2)\left[4(p_2^2-p_1^2)\cos^2\eta+5p_1^2-4p_1p_2\right]^{1/2}}{4(p_2^2-p_1^2)\cos^2\eta+(p_2-2p_1)^2}$
Tension Tension Compression	$f = \sigma_i, \quad i = 1, 2$ $s = \frac{f_t}{f_c}(1+\frac{\sigma_3}{f_c})$
Tension Tension Tension	$f = \sigma_i, \quad i = 1, 2, 3$ $s = \frac{f_t}{f_c}$

3.3.3. Stability constraints

Central angle of the arch: In this paper, constraints ensuring the sliding stability of the dam may be expressed by central angle of the arch.

$$1-\frac{\phi_U}{90} \leq 0, \qquad \frac{\phi_U}{110}-1 \leq 0, \tag{50}$$

$$1-\frac{\phi_D}{90} \leq 0, \qquad \frac{\phi_D}{110}-1 \leq 0, \tag{51}$$

where (ϕ) is the sum of central angles at the right and the left archs, and $90 \leq \phi_U \leq 110$, $90 \leq \phi_D \leq 110$.

Overturning: To verify the overall overturning stability of crown cantilever arch dam monoliths:

$$\mathrm{USP}_1 < Y_{\mathrm{bar}} \rightarrow \frac{\mathrm{USP}_1}{Y_{\mathrm{bar}}}-1 \leq 0. \tag{52}$$

4. Optimization algorithm

The Simultaneous Perturbation Stochastic Approximation (SPSA) has recently attracted considerable attention in areas, such as statistical parameter estimation, feedback control, simulation-based optimization, signal and image processing, and experimental design. However, the SPSA has not been tested yet for structural optimization and this is the first study employed for the purpose. The promising feature of the SPSA optimization algorithm is that it requires only two structural analyses in each cycle of optimization process, regardless of the optimization problem dimensions. This attribute can drastically reduce the computational cost of the optimization, particularly in problems with a number of variables to be optimized. The following step-by-step summary shows the process of SPSA in arch dam optimization:

Step 1. Initialization and coefficient selection. Set counter index $k = 0$. Pick initial guess and non-negative coefficients a, c, A, α, and γ in the SPSA gain sequences $a_k = a/(A+k+1)^\alpha$ and $c_k = c/(k+1)^\gamma$. The choice of gain sequences (a_k and c_k) is critical to performance of SPSA. Spall provides some guidance on picking these coefficients in a practically effective manner;

Step 2. Generation of the simultaneous perturbation vector. Generate an n_v dimensional random perturbation vector Δ_k by Monte Carlo, where each of the n_v components of Δ_k is independently generated from a zero mean probability distribution satisfying some conditions. A simple and theoretically valid choice for each component of Δ_k is using a Bernoulli ± 1 distribution with probability of $1/2$ for each ± 1 outcome. Note that uniform and normal random variables are not allowed for the element in Δ_k by the SPSA regularity conditions;

Step 3. Fitness function evaluations. Obtain two measurements of the fitness function $f(0)$ based on the simultaneous perturbation around the current design vector $\hat{x}_k$: $f(\hat{x}_k + c_k\Delta_k)$ and $f(\hat{x}_k - c_k\Delta_k)$ with the c_k and Δ_k from Steps 1 and 2;

Step 4. Gradient approximation. Generate the simultaneous perturbation approximation with the unknown accurate gradient $G(\hat{x}_k)$:

$$G_k(\hat{x}_k) \cong \widehat{G_k}(\hat{x}_k) = \frac{f(\hat{x}_k + c_k\Delta_k) - f(\hat{x}_k - c_k\Delta_k)}{2c_k}$$

$$\begin{bmatrix} \Delta_{k1}^{-1} \\ \Delta_{k2}^{-1} \\ \vdots \\ \Delta_{knv}^{-1} \end{bmatrix}, \tag{53}$$

where Δ_{ki} is the ith component of Δ_k vector;

Step 5. Updating $\hat{x}$ estimate. Use the standard Stochastic Approximation (SA) to update $\hat{x}_k$ to a new value $\hat{x}_{k+1}$:

$$\hat{x}_{k+1} = \hat{x}_k - a_k \widehat{G_k}(\hat{x}_k); \tag{54}$$

Step 6. Iteration or termination. Return to Step 2 with $k+1$ replacing k. Terminate the algorithm if the Maximum Number of Iterations (MNI) has been reached [28]. The flow chart of SPSA algorithm for the arch dam optimization problem can be shown in Figure 11.

5. Result

The optimization process of arch dam according to the above methodology converged after 1000 iterations.

Figure 12 shows the evolution of crown cantilever shape. The initial and optimum values of shape design variables are given in Table 5 (all dimensions are in meters). As can be seen, the volume of the dam body defined by the present optimization is 1057550 m^3 less than the initial volume, i.e. 21% less.

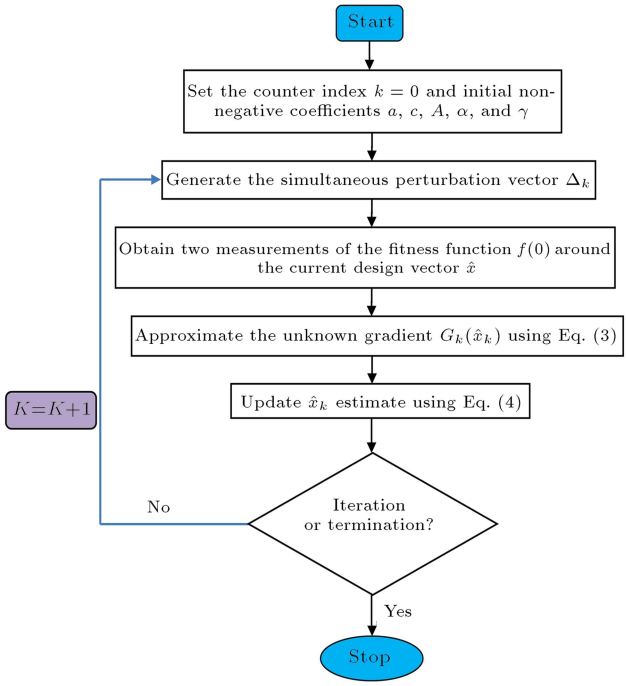

Figure 11. The flowchart of SPSA algorithm.

Table 5. Initial and optimum values of shape design variables.

		840	**725**	**625**	**515**
TC	Initial design	10	33.22	44.52	50
	Optimum design (iteration:1000)	8.48	24.67	34.60	45.80
T_{AL}	Initial design	10	48.87	60.1	50
	Optimum design	10.69	40.67	70.24	60.84
T_{AR}	Initial design	10	48.87	60.1	50
	Optimum design	9.49	41.66	67.34	52.65
USP	Initial design	63.12	18.65	6.83	20.00
	Optimum design	57.36	14.30	5.42	26.35
RLUS	Initial design	200.00	144.56	115.07	100.00
	Optimum design	194.54	128.88	108.32	100.72
RRUS	Initial design	200.00	144.56	115.07	100.00
	Optimum design	203.23	130.45	108.67	91.77
RLDS	Initial design	192.03	95.32	60.81	50.83
	Optimum design	192.37	105.56	70.47	49.99
RRDS	Initial design	192.03	94.98	61.48	50.83
	Optimum design	199.03	105.76	70.50	50.52

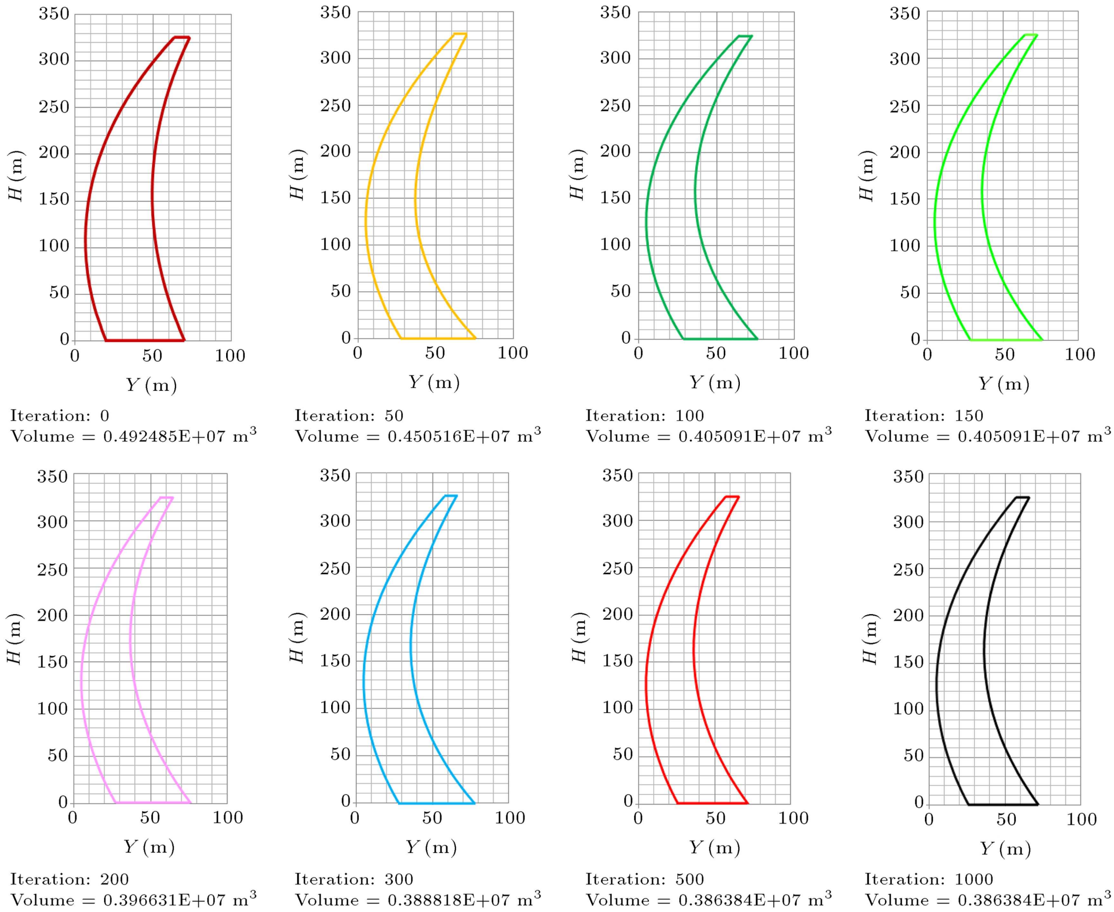

Figure 12. Shapes of crown cantilever at different numbers of iteration.

The difference between the initial and optimum design shapes can be seen in Figure 13. It is observed that the optimal design is thinner than the initial design and slope of overhang in upstream and downstream of surfaces in the optimum design are smaller than those of the initial design, which are benefits for construction [34].

The boldness coefficient in Table 6 is calculated by Lombardi's formula, as follows:

$$\text{Boldness coefficient} = \frac{\text{Mid surface area}^2}{(\text{Height of dam}) \times \text{volume}}. \tag{55}$$

The boldness coefficients for the initial and optimum designs are shown in Table 6. The boldness coefficient for the optimum design is higher than that for the initial design.

The principal stresses for two load cases are shown in Figure 14 and Table 7. The position of maximum tensile stress is found close to the one third of dam height. The maximum tensile stresses are obtained for the U/S face in two cases SUN1 and SU1. For the case of SUN1, the maximum compression stress is observed in the U/S face and for the case the SU1, it is obtained in the D/S case.

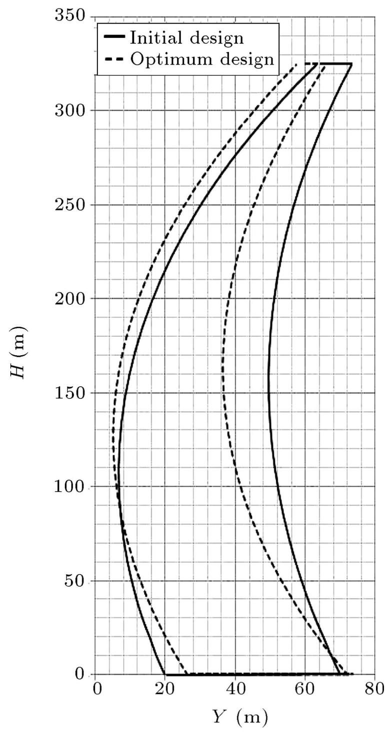

Figure 13. Comparison of shape crown cantilevers in the initial and optimum designs.

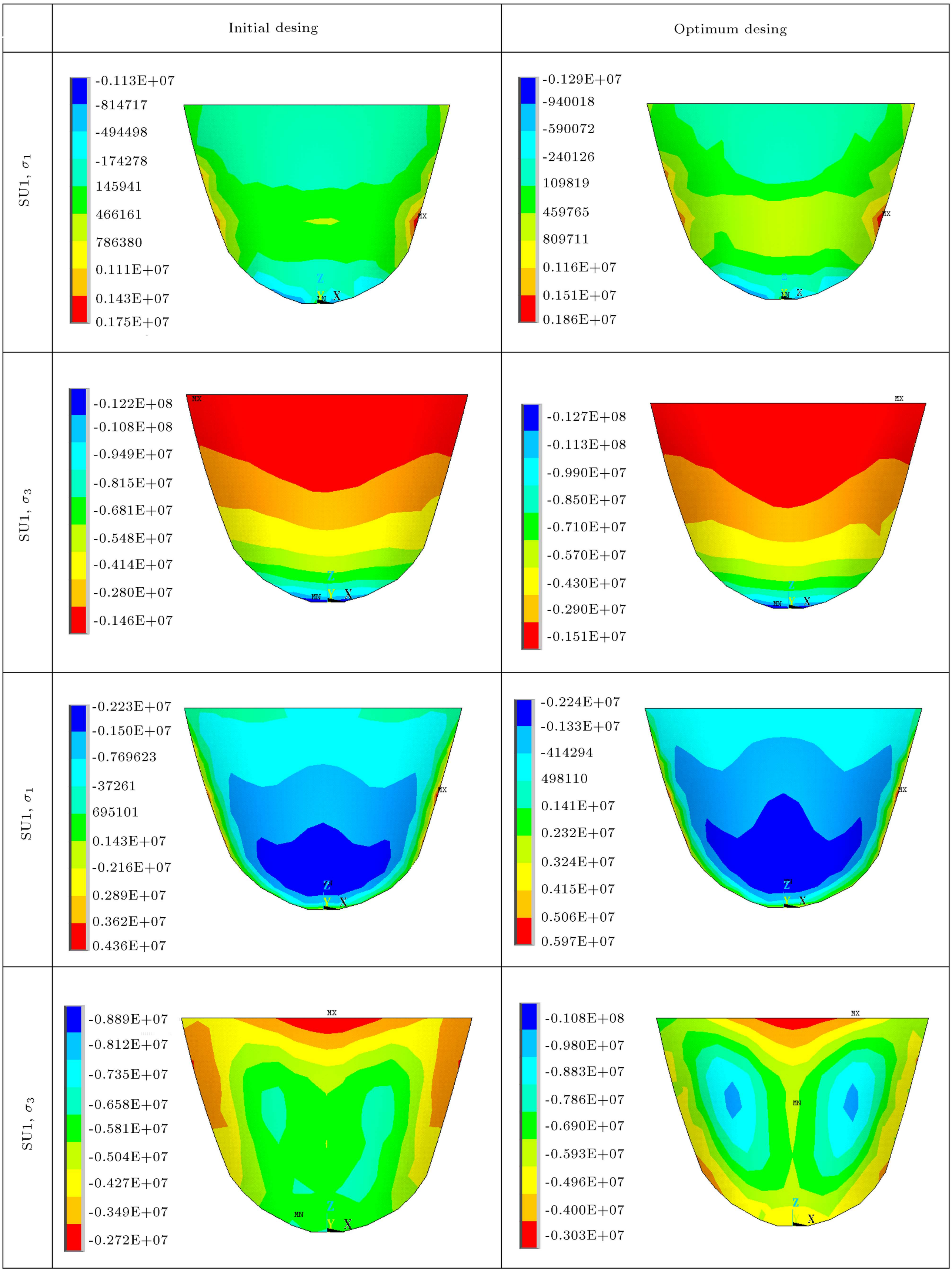

Figure 14. Principal stresses σ_1 and σ_3 in the initial and optimum design shapes for usual load combination (SU) and unusual load combination (SUN).

Table 6. Boldness coefficients for the initial and optimum designs.

Lombardi boldness coefficient (λ)				
Design	**Height (m)**	**Volume (m^3)**	**Mid surface area (m^2)**	λ
Initial design	325	4.924.850	137314	11.78
Optimum design	325	3.863.840	137972	15.16

Table 7. Summary of the results of the models.

		US		DS	
		Maximum tension	**Maximum compression**	**Maximum tension**	**Maximum compression**
Initial design	SUN1	1.72	-12.5	0.77	-4.26
	SU1	4.3	-7.43	2.12	-8.99
Optimum design	SUN1	1.85	-13	1.5	-4.4
	SU1	6.12	-9.9	3.3	-10.9

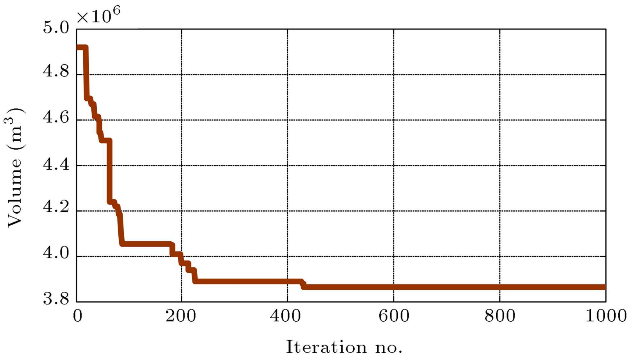

Figure 15. Convergence rate of the dam body volume.

The values of stresses for the optimum design are bigger than those for the initial design.

Convergence rate of the objective function in the optimization process is shown in Figure 15.

After performing the optimization process, the dam volume decreased by 21% in comparison with that in the initial design.

6. Conclusion

This paper employs a methodology to develop the interface between a finite element method and optimization algorithm for shape optimization of double curvature concrete arch dam.

In order to create the geometry of arch dams, a new algorithm is proposed in MATLAB. This algorithm is able to model the different shapes of an arch dam. The finite element of software ANSYS is taken for modeling the geometry of an arch dam used to consider the effects of dam body dead weight and upstream hydrostatic pressures. The following conclusions, some of which are important, are drawn from the present work:

- It is concluded that SPSA can be effectively used in the shape optimization of arch dams;
- Arch dam is a massive structure and therefore, its construction is staged into a step by step procedure. If the dead load is applied to the dam all at once, without taking into account the fact that horizontal load transfer cannot occur before the dam is complete, fictitious stresses will be indicated. By considering stage construction, there have been longer optimization process and lower optimum volume;
- The maximum tensile stresses are obtained for the U/S face in two cases SUN1 and SU1. For the case of SUN1, the maximum compression stress is observed in the U/S face and for the case of SU1, it is obtained in the D/S case. After the shape optimization of the arch dam, the dam body volume is reduced by 21%.

References

1. Grigorov, S., Tasev, S., Tzenkov, A., Fanelli, M. and Gunn, R. "Arch dam shape optimization procedure accounting for dam seismic response", *Proceedings of the 11th National Congress on Theoretical and Applied Mechanics* (2009).
2. Fialho, J.F.L. "Leading principles for the design of arch dams", *A New Method of Tracing and Dimensioning*, LNEC, Lisbon, Portugal (1955).
3. Serafim, J.L. "New shapes for arch dams", *Civil Engineering, ASCE*, **36**(2) (1966).
4. Rajan, M.K.S., *Shell Theory Approach for Optimization of Arch Dam Shapes*, University of California, Berkeley (1968).
5. Sharpe, R. "The optimum design of arch dams", *Proceedings of the ICE - Civil Engineering*, Supplementary Volume, pp. 73-98 (1969).

6. Ricketts, R.E. and Zienkiewicz, O.C. "Shape optimization of concrete dams", *Criteria and Assumptions for Numerical Analysis of Dams*, Quadrant Press, Swansea, London, UK, pp. 1179-1206 (1975).

7. Mohr, G.A. "Design of shell shape using finite elements", *Computers & Structures*, **10**(5), pp. 745-749 (1979).

8. Sharma, R. "Optimal configuration of arch dams", Ph.D. Thesis, Indian Institute of Technology, Kanpur (1983).

9. Rahim, A.S. "Optimum shape of an arch dam for static loads", MEng Thesis, Asian Institute of Technology, Bangkok (1983).

10. Wasserman, K. "Three dimensional shape optimization of arch dams with prescribed shape function", *Journal of Structural Mechanics*, **11**(4), pp. 465-489 (1984)

11. Li, Y. and Bofang, Z. "The optimum design of arch dams and the curve of arch thickness", *Journal of Hydraulic Engineering*, CNKI (1985).

12. Bofang, Z. "Shape optimization of arch dams", *Int. Water Power Dam Construct.*, **39**(3) pp. 43-51 (1987).

13. Samy, M.S. and Wieland, M. "Shape optimization of arch dams for static and dynamic loads", in *Proceedings of International Workshop on Arch Dams*, Coimbra (1987).

14. Yao, T.M. and Choi, K.K. "Shape optimal design of an arch dam", *Journal of Structural Engineering, ASCE*, **115**(9), pp. 2401-2405 (1989).

15. Guohua, L. and Shuyu, W. "Optimum design of concrete arch dam", *Proc. Int. Concrete Conf.*, Tehran, pp. 444-452 (1990).

16. Simões, L.M.C., Lapa, J.A.M. and Negrao, J. "Search for arch dams with optimal shape", In *Arch Dams*, pp. 99-114 (1990).

17. Bofang, Z. "Optimum design of arch dams", *Dam Eng. I*, **2**, pp. 131-145 (1990).

18. Bofang, Z., Rao, B., Jia, J. and Li, Y. "Shape optimization of arch dams for static and dynamic loads", *J. Struct. Eng., ASCE*, **118**(11), pp. 2996-3015 (1992).

19. Bofang, Z., Jinsheng, J., Rao, B. and Yisheng, L. "Mathematical models for shape optimization of arch dams", *Journal of Hydraulic Engineering* (1992).

20. Fanelli, A., Fanelli, M. and Salvaneschi, P. "A neural network approach to the definition of near optimal arch dam shape", *Dam Eng.*, **4**(2), pp. 123-140 (1993).

21. Guohua, L. and Shuyu, W. "Methods and applications of arch dam optimization", *Chinese Journal of Computational Mechanics* (1994).

22. Yisheng, L. "The optimum type of ring for arch dam", *Journal of Hydraulic Engineering* (1996).

23. Sun, L.S., Zhang, W.H. and Guo, X.W. "Shape optimization of arch dams based on accelerated micro genetic algorithm", *Journal of Hohai University: Natural Sciences*, **36**(6), pp. 758-762 (2008).

24. Li, S., Ding, L., Zhao, L. and Zhou, W. "Optimization design of arch dam shape with modified complex method", *Advances in Engineering Software*, **40**(9), pp. 804-808 (2009).

25. Fanelli, A. "Some remark on shape optimization of arch dams", *Mathematical Modeling in Civil Engineering*, **5** (2009).

26. Peng, H., Yao, W. and Huang, P. "The application of genetic algorithm to closure temperature fields and shape optimization of Jinping high arch dam", In *2010 Sixth International Conference on Natural Computation*, **5**, pp. 2489-2493 (2010).

27. Tajalli, F., Ahmadi, M.T. and Moharrami, H. "A shape optimization algorithm for seismic design of a concrete arch dam. Dam Engineering", *Dam Engineering*, **18**(2) (2007).

28. Seyedpoor, S.M., Salajegheh, J., Salajegheh, E. and Gholizadeh, S. "Optimal design of arch dams subjected to earthquake loading by a combination of simultaneous perturbation stochastic approximation and particle swarm algorithms", *Applied Soft Computing*, **11**(1), pp. 39-48 (2011).

29. Akbari, J., Ahmadi, M.T. and Moharrami, H. "Advances in concrete arch dams shape optimization", *Applied Mathematical Modeling*, **35**(7), pp. 3316-3333 (2011).

30. Takalloozadeh, M. and Ghaemian, M. "Shape optimization of concrete arch dams considering abutment stability", *Scientia Iranica*, **21**(4), pp. 1297-1308 (2014).

31. Abraham, S. and Narayanan, K.V. "Definition of geometry of variable radius arch dam with degree of polynomial in the 3D finite element analysis", In *Proceedings of the 10th WSEAS (World Scientific and Engineering Academy and Society) International Conference on Mathematical and Computational Methods in Science and Engineering*, pp. 133-136 (2008).

32. Hollerbuhl, L. "Crack propagation simulations for the Koelnbrein-Dam 1978" [Simulation der Schädigung der Kölnbreintalsperre während des Ersteinstaus 1978], M.S. Thesis, Bauhaus-Universität Weimar, German (2005).

33. Boggs, H.L., *Guide for Preliminary Design of Arch Dams*, US Department of the Interior, Bureau of Reclamation, **36** (1966).

34. Zhang, X.-f., Li, S.-y. and Chen, Y.-l. "Optimization of geometric shape of Xiamen arch dam", *Advances in Engineering Software*, **40**(2), pp. 105-109 (2009).

Biographies

Somayyeh Pourbakhshian is a PhD degree candidate in Civil Engineering Department, Science and Research Branch, Islamic Azad University, Tehran, Iran. Her research interests are mathematical methods in optimization, shape and topology optimization of structures, and sensitivity analysis. In recent years, she has been working on shape optimization of concrete dam.

Mohsen Ghaemian is Professor in Civil Engineering Department at Sharif University of Technology, Tehran, Iran. His current research activities include dynamic responses of gravity and arch dams, dam reservoir interaction effects, seismic response of dams due to non-uniform excitations, and nonlinear behavior of concrete dams.

Abdolreza Joghataie is Faculty Member in Civil Engineering Department at Sharif University of Technology, Tehran, Iran. His research interests include application of neural networks in different areas of structural engineering, including nonlinear dynamic analysis of dams.